The Journal of Experimental Biology 213, 2430-2443

doi:10.1242/jeb.037820

The ultrastructure and contractile properties of a fast-acting, obliquely striated, myosin-regulated muscle: the funnel retractor of squids

Jack Rosenbluth[1], Andrew G. Szent-Györgyi[2] and Joseph T. Thompson[3,*]

[1]Department of Physiology and Neuroscience and Rusk Institute, School of Medicine, New York University, New York, NY 10016, USA, [2]Rosenstiel Basic Medical Sciences Research Centre, Brandeis University, Waltham, MA 02454, USA and [3]Department of Biology, Franklin and Marshall College, PO Box 3003, Lancaster, PA 17604-3003, USA

*Author for correspondence (joseph.thompson@fandm.ed)

Accepted 9 April 2010

SUMMARY

We investigated the ultrastructure, contractile properties, and *in vivo* length changes of the fast-acting funnel retractor muscle of the long-finned squid *Doryteuthis pealeii*. This muscle is composed of obliquely striated, spindle-shaped fibers ~3 μm across that have an abundant sarcoplasmic reticulum, consisting primarily of membranous sacs that form 'dyads' along the surface of each cell. The contractile apparatus consists of 'myofibrils' ~0.25–0.5 μm wide in cross section arrayed around the periphery of each cell, surrounding a central core that contains the nucleus and large mitochondria. Thick myofilaments are ~25 nm in diameter and ~2.8 μm long. 'Dense bodies' are narrow, resembling Z lines, but are discontinuous and are not associated with the cytoskeletal fibrillar elements that are so prominent in slower obliquely striated muscles. The cells approximate each other closely with minimal intervening intercellular connective tissue. Our physiological experiments, conducted at 17°C, showed that the longitudinal muscle fibers of the funnel retractor were activated rapidly (8 ms latent period following stimulation) and generated force rapidly (peak twitch force occurred within 50 ms). The longitudinal fibers had low V_{max} (2.15 ±0.26 L_0 s^{-1}, where L_0 was the length that generated peak isometric force) but generated relatively high isometric stress (270±20 mN mm^{-2} physiological cross section). The fibers exhibited a moderate maximum power output (49.9 W kg^{-1}), compared with vertebrate and arthropod cross striated fibers, at a V/V_{max} of 0.33±0.044. During ventilation of the mantle cavity and locomotion, the funnel retractor muscle operated *in vivo* over a limited range of strains (+0.075 to –0.15 relative to resting length, L_R) and at low strain rates (from 0.16 to 0.91 L_R s^{-1}), corresponding to a range of V/V_{max} from 0.073 to 0.42. During the exhalant phase of the jet the range of strains was even narrower: maximum range less than ±0.04, with the muscle operating nearly isometrically during ventilation and slow, arms-first swimming. The limited length operating range of the funnel retractor muscles, especially during ventilation and slow jetting, suggests that they may act as muscular struts.

Key words: cephalopod, obliquely striated muscle, muscular strut, myosin regulation.

INTRODUCTION

Actin-linked regulation of force production *via* binding of Ca^{2+} to troponin C, the accompanying conformational change by tropomyosin to reveal myosin binding sites along the actin filament, and subsequent crossbridge cycling in the presence of ATP are familiar from studies of vertebrate striated muscles (Ebashi et al., 1969; Eisenberg and Kielley, 1970; Weber and Murray, 1973). In the muscles of numerous invertebrates regulation occurs *via* binding of Ca^{2+} to the essential light chain of myosin [which contains the ligands for Ca^{2+} but requires stabilization by the regulatory light chain of the myosin molecule (Xie et al., 1994; Fromherz and Szent-Györgyi, 1995; Houdusse et al., 2000) (for a review, see Szent-Györgyi, 2007)]; in fact, regulation is dominated by myosin (Lehman and Szent-Györgyi, 1975; Simmons and Szent-Györgyi, 1978). Thus, these muscles are termed, 'myosin regulated'.

Myosin-linked regulation appears to be common among invertebrate muscles, and its distribution across disparate taxa (see Lehman and Szent-Györgyi, 1975) suggests that it evolved several times independently. Indeed, muscles with myosin-linked regulation may be more widespread phylogenetically than muscles whose contraction is regulated *via* the thin filament alone. Among muscles with myosin-linked regulation, only the funnel retractor of the long-finned squid *Doryteuthis* (formerly *Loligo*) *pealeii* and the striated adductor of scallops (*Argopecten irradians* and *Placopecten magellanicus*) have been studied in detail at the atomic and molecular levels, and such studies have revealed remarkable similarities in the myosins. The atomic structure of the S1 motor domains with the lever arm of the scallop (Houdusse et al., 1999) and squid (Yang et al., 2007) muscles is very similar. The lever arms, which are extensions of the motor domains, are responsible for movement and regulation by binding calcium in both species. In addition, the steady state ATPase activities of the S1 head are "unusually high" (Yang et al., 2007), and also are similar in the scallop and squid muscles: 0.50±0.05 mol s^{-1}, 0.45±0.03 mol s^{-1} and 0.64±0.05 mol s^{-1} for *D. pealeii*, *A. irradians* and *P. magellanicus*, respectively [(Perreault-Micale et al., 1996) and supplemental data in Yang et al. (Yang et al., 2007)]. It is noteworthy that measurement of ATPase activity of heavy meromyosin (HMM) can be followed kinetically and accounts for the major portion of the activity without actin (Wells and Bagshaw, 1985). Finally, HMM purified from the scallop and squid muscles has very high Ca^{2+} affinity (Lehman and Szent-Györgyi, 1975; Kalabokis and Szent-Györgyi, 1997) (L. O'Neall-Hennesey, personal communication).

The biochemical studies of scallop myosin have been accompanied by investigations into the contractile properties of the striated adductors in *A. irradians* and *P. magellanicus* (Rall, 1981; Olson and Marsh,

1993; Marsh and Olson, 1994). However, the contractile properties of the funnel retractor muscles of squids have received less exhaustive attention. The paired funnel retractors [also known as the depressor infundibuli (Williams, 1909) and retractor infundibuli (Young, 1938)] of squids are large and impressive muscles (Fig. 1) that originate on the chitinous gladius of the mantle about one-half of the dorsal mantle length from the anterior edge of the mantle and insert on the posterolateral portions of the funnel (Williams, 1909). The funnel retractor muscles of *D. pealeii* are composed of both longitudinal and transverse muscle fibers (Young, 1938), and their muscle and connective tissue organization is consistent with that of a muscular hydrostat (Kier and Thompson, 2003) [see Kier and Smith (Kier and Smith, 1985) for discussion of muscular hydrostats]. The muscle fibers have been described as 'helical smooth' without I zones or Z lines (Hanson and Lowy, 1957), but here we show that the fibers have all of the structural characteristics of obliquely striated fibers. The function of the funnel retractor muscles is unknown but based on their position within the body, they may serve to stabilize the base of the funnel (Fig. 1) during jet locomotion (Kier and Thompson, 2003).

Objectives

Our aim was to compare the funnel retractor muscle of *D. pealeii* to another fast-acting myosin-regulated muscle, the striated adductor of the scallop, studied previously, with respect to ultrastructure, contractile properties and *in vivo* function.

The high Ca^{2+} affinity and ATPase activity of the myosins of the respective squid and scallop muscles suggest that they may be activated rapidly, develop force rapidly and shorten at high velocities. Studies of *A. irradians* and *P. magellanicus* confirm that their striated adductors are activated rapidly and that they shorten rapidly (Rall, 1981; Olson and Marsh, 1993). Thus, we predicted that the longitudinal fibers of the funnel retractor muscles would similarly be activated rapidly (i.e. have a short latent period, T_L, between stimulation and the onset of force production) and exhibit a rapid rise in force (i.e. a short time, T_P, between the onset of force production and the peak force). Furthermore, if the longitudinal fibers of the funnel retractor muscles are activated rapidly, as are the striated adductors of scallops, then it is reasonable to speculate that rapid activation would be coupled with a rapid Ca^{2+} delivery system. Therefore, we also predicted that the longitudinal fibers of the funnel retractor muscles have abundant sarcoplasmic reticulum. Finally, there is a strong correlation between ATPase activity of the myosin heavy chain and maximum unloaded shortening velocity (V_{max}) of the fiber in vertebrate striated muscles (Bárány, 1967). Moreover, there is an inverse relationship between T_P and V_{max} (Close, 1965). Given the high ATPase activity of funnel retractor myosin [supplemental data in Yang et al. (Yang et al., 2007)] and the predicted short T_P, we predicted that the longitudinal fibers of the funnel retractor muscles have a high V_{max}.

MATERIALS AND METHODS

We tested our predictions using sexually mature adult long-finned squid *Doryteuthis pealeii* Lesueur 1821. The staff of the Marine Resources Center at the Marine Biological Laboratories (Woods Hole, MA, USA) provided nine of the animals used for the morphological studies. We captured male and female *D. pealeii* at night from lighted piers in South Bristol and Walpole, Maine, USA, using a 4.2 m diameter cast net, for the muscle physiology (n=10) and sonomicrometry (n=4) experiments. We used only squid that had no visible damage to the skin or mantle and that appeared to be completely healthy. The animals ranged in size from 110 to 260 mm dorsal mantle length.

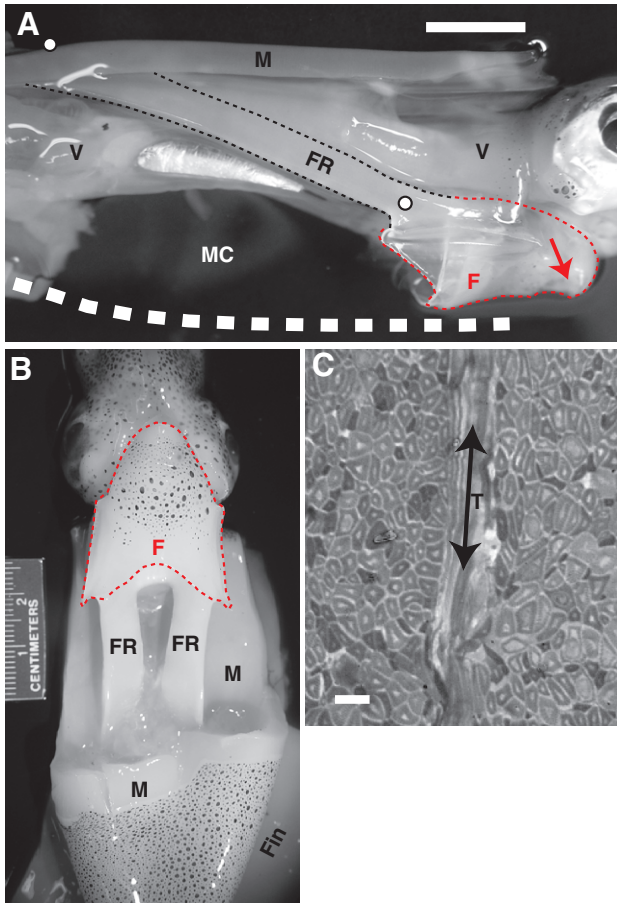

Fig. 1. (A) Right side of a small adult long-finned squid *Doryteuthis pealeii* illustrating the right funnel retractor muscle (FR, black dashed line) and the funnel (F, red dashed line). Part of the right eye is visible at the right edge of the photo; the tail is to the left. Most of the mantle (M) was removed but a portion of the dorsal mantle (top) is visible. The dashed white line indicates the approximate position of the ventral edge of the mantle and the enclosed mantle cavity (MC). The arrow indicates the funnel aperture, although the aperture is closed in the photograph. White circles indicate the two sonomicrometry crystals. V, viscera. Scale bar, 1 cm. (B) Ventral view of the funnel (F) and funnel retractor muscles (FR). The head and arms are at the top of the photo; the tail and fins toward the bottom. (C) Bright-field photomicrograph of a cross section of the funnel retractor muscle showing a bundle of transverse muscle fibers (T, arrow indicates long axis) and the longitudinal muscle fibers. The lightly stained region at the center of each longitudinal fiber is a core of mitochondria. Scale bar, 5 μm.

Muscle mechanical testing

We focused on the longitudinal fibers of the funnel retractor muscles because they make up the majority of the volume of the muscles (Kier and Thompson, 2003) and, therefore, are probably the source of myosin in the structural and biochemical studies described in the Introduction. Each squid was anesthetized in cold seawater (3–5°C) (O'Dor and Shadwick, 1989; Bower et al., 1999) and killed by decapitation. We removed one entire funnel retractor muscle by first slicing through the muscle at its origin on the gladius (the 'pen') and its insertion on the funnel, and then carefully cutting the fascia connecting the muscle to the viscera and dorsal wall of the mantle (Fig. 1). We glued the dorsolateral region of the muscle with Vetbond (3M, St Paul, MN, USA) to the temperature-controlled stage of a Vibratome. Immediately after gluing, the bath surrounding the stage was filled with a modified squid saline solution at 3–4°C

containing (in mmol l^{-1}): NaCl (450), $MgCl_2 \cdot 6H_2O$ (10), Hepes (10), EGTA (10), pH adjusted to 7.8 with 2 mol l^{-1} NaOH (Milligan et al., 1997).

We used the vibratome to slice the muscle in half along its long axis and then cut sheets of muscle 0.1–0.2 mm thick. The vibratome severed and thus disabled the transverse muscle fibers, which were oriented perpendicular to the section plane (see Kier and Thompson, 2003). The sheets were composed primarily of intact longitudinal muscle fibers (i.e. those fibers that run parallel to the long axis of the funnel retractor muscle), although fragments of both transverse muscle fibers and connective tissue fibers were also present.

The muscle sheets were cut into preparations 8–12 mm long and 2–4 mm wide. T-shaped foil clips (Milligan et al., 1997) were glued to each end of the preparation using Vetbond and then the preparation was transferred to a temperature-controlled muscle bath. The muscle bath was filled with standard squid saline at 17°C containing (in mmol l^{-1}): NaCl (470), KCl (10), $CaCl_2$ (10), $MgCl_2 \cdot 6H_2O$ (50), glucose (20), Hepes (10), pH adjusted to 7.8 with 2 mol l^{-1} NaOH (Milligan et al., 1997). The muscle preparations were allowed to equilibrate in the standard squid saline for 60 min prior the start of an experiment.

The muscle preparations were fixed at one end and attached at the other to an ASI 300B muscle lever system (Aurora Scientific Inc., Aurora, ON, Canada). The muscle lever allowed us to conduct both isotonic and isometric tests on the muscle preparations.

We stimulated the muscle preparations with rectangular constant current pulses *via* platinum plate electrodes that were of sufficient size to cover the length of preparation. The length–force relationship of the preparation was determined using supramaximal, brief tetanic (2 ms pulses, 50 Hz, 200 ms duration, 300 s between successive tetani) and twitch stimulations (180 s between successive twitches). Once we determined the length (L_0) of the preparation that yielded peak tetanic force (P_0), we next studied the stimulus frequency–force relationship using brief tetani (2 ms pulse, 200 ms duration, 300 s between successive tetani) at a range of frequencies between 1 and 500 Hz. We calculated the peak tetanic stress of the fibers by dividing P_0 by the physiological cross section of the preparation (see following section for details). With the preparation maintained at L_0, we then determined the force–velocity relationship in brief tetanus. Isotonic shortening of the preparation was accomplished with the muscle lever in force–clamp mode. We fitted Hill's equation (Hill, 1938) to the force–velocity data using the Solver function of Microsoft Excel to minimize the sum of the squares of the deviations of predicted velocity from the observed velocity (Kier and Curtin, 2002). The form of the equation was:

$$V = V_{max} P^* (P^* - P) / (GP + 1) , \quad (1)$$

where V is the shortening velocity ($L_0\,s^{-1}$), P is the force during shortening relative to peak isometric force, V_{max} is the intercept on the velocity axis, P^* is the intercept on the force axis, and G is the constant expressing curvature of the force–velocity relationship (Hill, 1938) (for details, see Kier and Curtin, 2002). All data points for each squid were given equal weighting and the hyperbolic curve fitting was not constrained to pass through P=1.0.

We also analyzed two temporal aspects of the brief tetanic contraction at L_0. First, we measured the latent period (T_L) as the time from the beginning of the first rectangular pulse stimulation to the initial rise in force. Second, we measured the time to peak (T_P) as the time from the initial rise in force to the peak force produced.

We performed periodic isometric control stimulations to monitor the health of the preparation. If the force produced during isometric contraction at L_0 decreased by more than 10%, we terminated the experiment and discarded all data collected subsequent to the previous control stimulation.

Morphology methods

Immediately following the mechanical testing, the muscle preparations were fixed at L_0 at 4°C in 3.0% glutaraldehyde, 0.065 mol l^{-1} phosphate buffer, 0.5% tannic acid and 6% sucrose for 12–24 h and then postfixed for 45 min at 4°C in a 1:1 solution of 2% osmium tetroxide and 2% potassium ferrocyanide in 0.13 mol l^{-1} cacodylate buffer (Kier, 1985). A small block at the center of the preparation (that included the entire cross section of the preparation) was excised, rinsed in chilled 0.13 mol l^{-1} cacodylate buffer for 30 min, dehydrated in a graded series of acetones and embedded in epoxy resin for determination of physiological cross section. The remainder of the preparation was saved for post-fixation, processing, and EM analysis (described below).

For physiological cross section determination, 1-μm thick transverse sections of the preparations were cut and stained with an aqueous solution of 1% Toluidine Blue and 1% sodium borate. The stained slides were photographed under bright-field microscopy. Both the total cross-sectional area of the preparation and the portion occupied by the transverse muscle fibers were measured using ImageJ (public domain software; National Institutes of Health, USA). We then subtracted the area of all the transverse muscle fibers in the preparation from the total cross-sectional area of the preparation to obtain the physiological cross section of the longitudinal muscle fibers. The physiological cross section, therefore, included the areas occupied by the myofilaments, the cores of mitochondria, and the other cellular components of the longitudinal muscle fibers, but not the portions of the preparation occupied by the transverse muscle fibers.

For the ultrastructural analysis, the remains of nine of the aldehyde-fixed muscle preparations were cut into pieces no thicker than 1 mm for either cross or longitudinal sectioning, rinsed, post-fixed in 1–2% osmium tetroxide in 0.1 mol l^{-1} cacodylate buffer with or without 1.5% added potassium ferricyanide, dehydrated in a graded series of methanol solutions and 100% propylene oxide, infiltrated and embedded in Araldite. Thick (1 μm) and thin (0.1 μm) sectioning was carried out with a Dupont-Sorvall MT2 ultramicrotome. Thick sections were stained with alkaline Toluidine Blue for light microscopic examination. Thin sections were stained with potassium permanganate and uranyl acetate and examined with a Philips or JEOL electron microscopic at 60 or 80 kV at NYU School of Medicine.

Nine additional squid from the Marine Biological Laboratories were killed by decapitation and used for morphological studies. The funnel retractor muscles were either excised and immersed in fixative or injected with fixative *in situ*, in some cases with the muscle under stretch. Primary fixation was carried out with either glutaraldehyde or glutaraldehyde–formaldehyde. The glutaraldehyde fixative consisted of 4, 6 or 12% glutaraldehyde in 0.05–0.1 mol l^{-1} cacodylate buffer (pH 7.4) made up in distilled water or in half-strength seawater. The glutaraldehyde–formaldehyde fixative consisted of 3.2% glutaraldehyde, 2% formaldehyde, 6% sucrose and 1.5% tannic acid in 0.1 mol l^{-1} cacodylate buffer.

Muscle length changes

We assessed *in vivo* length changes of the funnel retractor muscle using a sonomicrometer (Triton Technology Inc., San Diego, CA, USA). First, we anesthetized the squid in cold (3–4°C) seawater. We then attached one omnidirectional sonomicrometry crystal

(1.0 mm diameter; Sonometrics Corp., London, Ontario, Canada) to the junction of the funnel retractor muscle and the funnel, and a 2.0 mm diameter crystal (the 'pinger') to the dorsal surface of the mantle at the origin of the funnel retractor muscle on the pen (Fig. 1). Each transducer was attached with a superficial stitch of 7/0 polypropylene suture material. We also attached a second pair of omnidirectional transducers to the dorsal and ventral midline about one-third of the dorsal mantle length from the anterior edge of the mantle to correlate mantle activity during jetting with funnel retractor muscle length changes.

Following surgery, squid were transferred to a 2 m×1 m×0.5 m deep tank filled with natural seawater at 15–17°C. The squid recovered rapidly and then used combinations of jetting and fin movements to swim both forward and backward at a variety of speeds, from low amplitude jets that ventilated the mantle cavity to large amplitude escape jets. The analog output from the sonomicrometer was digitized (DI-158, Dataq Instruments, Akron, OH, USA) and recorded at 1 kHz. We used 1576 m s^{-1} as the speed of sound through the mantle (Goldman and Hueter, 1956) and corrected the sonomicrometer output accordingly (i.e. the calibration circuit of the sonomicrometer assumed a speed of 1520 m s^{-1}). We confirmed the output of the sonomicrometer periodically by attaching the transducers to linear translation stages equipped with micrometer adjustment screws, and generating our own calibration curves.

The speed of sound through the squid was probably lower than 1576 m s^{-1} because the 'line of sight' distance between the pinger and receiver included muscle tissue and water in the mantle cavity. Thus we slightly overestimated the speed of sound and, therefore, the muscle length changes we report below.

Each animal swam for up to 20 min before we terminated the experiment. For most jets, the animals stayed away from the sides of the tank but we excluded sequences in which the animals bumped into the side in case doing so affected mantle kinematics or funnel retractor muscle length changes. We also excluded sequences in which the animal turned during the jet.

Many squids, including the *D. pealeii* studied here, exhibit an impressive repertoire of fin, mantle and funnel movements during locomotion (e.g. O'Dor, 1988; Bartol et al., 2008). We focused on the behavior of the funnel retractor muscles during jetting, and thus reduced this locomotor diversity into three, qualitatively distinct categories. (1) 'Ventilation' in which the squid rested with only the tips of its arms and the posterior tip of its tail providing support on the bottom. During 'ventilation' the fins were quiescent and the squid used low amplitude contractions and expansions of the mantle to ventilate the mantle cavity. We have observed ventilation behavior in both the field and laboratory. (2) 'Slow swimming' in which the animal swam slowly [i.e. <1 dorsal mantle length (DML) s^{-1})] tail-first swimming (i.e. backward) or arms-first swimming (i.e. forward) using combinations of fin movements and jets. (3) 'Fast swimming' in which the squid swam tail or arms first using vigorous jets and fin movements. Fast swimming occurred at >3 DML s^{-1}. The transitions from ventilation to slow swimming to fast swimming were not gradual, and the sudden and dramatic increases in swimming speed made distinguishing between the categories easy. The swimming speeds we report for each category were obtained from the high-speed video records of a different study of jet locomotion in adult *D. pealeii* (J.T.T., P. S. Krueger and I. K. Bartol, unpublished data). In that study, squid exhibited two swimming speeds in large tanks in the lab: slow (always <1 DML s^{-1}) and fast (always >3 DML s^{-1}). Fast swimming included escape jetting, and both fast and slow swimming were readily distinguished by eye during the swimming trials, in addition to being confirmed from the high-speed video data (J.T.T., P. S. Krueger, I. K. Bartol, unpublished data). Although we did not collect synchronized high-speed video and sonomicrometry data for the trials reported here, we felt the clear demarcation between swimming speeds allowed us, at least as a first approximation, to assess how funnel retractor muscle behavior changed with swimming speed.

Following the swimming trial, we then killed each squid by over-anesthetizing it in an aqueous magnesium chloride solution (Messenger et al., 1985) and evaluated the alignment of the transducers.

We converted the muscle length changes to engineering strain as $(L_I–L_R)/L_R$ where L_I is the instantaneous distance between the transducers and L_R is the distance between the transducers with the funnel retractor muscle at rest. We measured L_R as the length at one half the amplitude of one elongation-shortening cycle during ventilatory movements of the mantle.

RESULTS

Transverse sections through the funnel retractor muscle show fibers that are ~3 μm across but vary in diameter, presumably reflecting their spindle shape. They are often polygonal in outline rather than round or oval, and they are closely packed together with very little intervening connective tissue between the individual muscle fibers where they are apposed (Fig. 2). This endomysial space, which is narrow, contains neither formed connective tissue elements, e.g. collagen fibrils, nor clear-cut basal laminae on the muscle cell plasma membranes. At 'corners', where three cells come together, the space widens, and there collagen bundles may be present (Fig. 2). The specimens used for physiological studies and fixed afterwards show some 'ghost' fiber profiles devoid of myofilaments, presumably the consequence of using a vibratome, alongside fibers that appear intact and well preserved. No 'ghost' fibers were seen in the muscles fixed *de novo*.

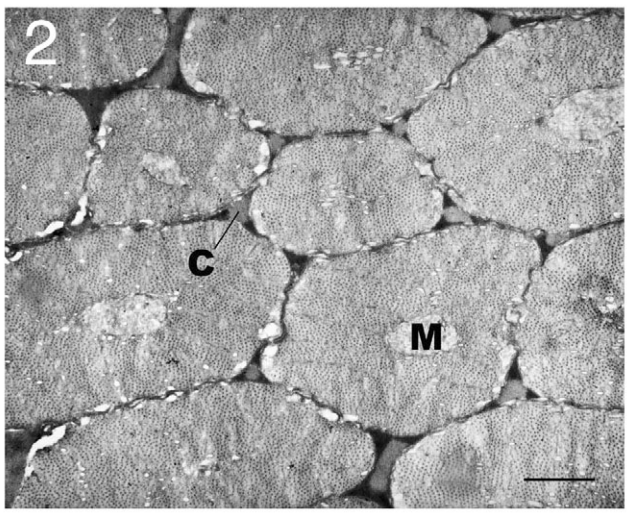

Fig. 2. Survey EM showing transversely sectioned muscle fibers. Those cut through their mid-regions are ovoid or polygonal in outline and ~3 μm across. Myofibrils are peripheral surrounding a central core of mitochondria (M) or the muscle cell nucleus (not shown). The fibers, which are outlined by ferricyanide (black), are closely apposed except at 'corners' where the space widens and sometimes contains a bundle of collagen fibrils (C). Scale bar, 1 μm.

Organization of the myofilaments

In cross sections, the fibers can be seen to contain ranks of filament bundles, ~0.25–0.50 μm across, around the periphery, surrounding a core that contains large mitochondria, granular ER and the cell nucleus (Fig. 2). In some cases a granular material consistent with glycogen can be seen also.

Each filament bundle consists of thick and thin filaments organized into arrays typical of those seen in other obliquely striated muscles (Hanson and Lowy, 1961; Knapp and Mill, 1971; Rosenbluth, 1965a; Rosenbluth, 1968). The bundles are oriented roughly perpendicular to the cell surface (Fig. 3) and consist of rows of five to ten thick filaments associated with thin filaments (A zones). Thin filaments are usually interspersed throughout the A zone, but in muscles that have been deliberately stretched during fixation, they may be absent from a narrow H zone in the middle of the A zone (Fig. 4), but are present more laterally on either side, where thick filaments are absent (I zone).

The filament bundles are typically separated from one another by radially oriented vesicular sacs extending inward from the periphery (Fig. 3). Linear fibrous structures are present in the same region consistent with Z-lines. These are, however, not always visible and are relatively less dense in this muscle compared with the prominent 'dense bodies', Z-line counterparts, in other obliquely striated muscles (Rosenbluth, 1965a). The Z lines in the funnel retractor muscle may have a considerable radial extent in the transverse plane, as they do in the body wall muscles of the annelids *Lumbricus terrestris* (Knapp and Mill, 1971) and *Glycera dibranchiata* (Rosenbluth, 1968), but they were not seen associated with the surface of the cell, differing markedly in that respect from dense bodies in other obliquely striated and smooth muscles (Rosenbluth, 1972). They differ also in that they are not associated with the prominent cytoskeletal elements present in other muscles.

Thick filaments (Fig. 4) are widest in the middle region (27.3±2.1 nm; ±s.d.) and thinnest near their ends (18.1±2.0 nm); overall, widths average 24.6±1.9 nm. Thin filaments are 8.8±0.9 nm, compared with 7–8 nm in vertebrate muscles, based on rotary shadowed, quick-frozen preparations (Fowler and Aebi, 1983). Since our measurements were made on transverse thin sections of fixed embedded material, our thin filament widths may appear increased as a result of obliquity or helical course of the filaments within the thickness of the 0.1 μm section or addition of osmium or ferricyanide molecules to the protein during fixation or of permanganate or uranyl salts during section staining. Reducing our thin filament measurements by 15% brings them into the same range as those obtained by negative staining.

Thick filament widths as well may appear to be increased because of the halo of cross bridges extending from them, superimposed within the thickness of the section, making the boundaries of the thick filament shafts indistinct (Fig. 5).

If we also reduce our measured thick filament widths by 15% this would bring their diameter down to ~21 nm, still clearly greater than the width of vertebrate myosin filaments but in the same range as that in other obliquely striated muscles (Hoyle, 1969). Differences in diameter could reflect differences in the packing of the myosin molecules or the presence of other proteins, e.g. paramyosin or calcium-sensitive regulatory proteins in the thick filaments. Neighboring thick filaments are spaced at intervals of 50.2±5.2 nm (±s.d.). Although in some cases they can be seen to be in regular hexagonal array (Fig. 5), usually they are less regular in their packing, perhaps because of disorder related to 'double overlap' of the thin filaments.

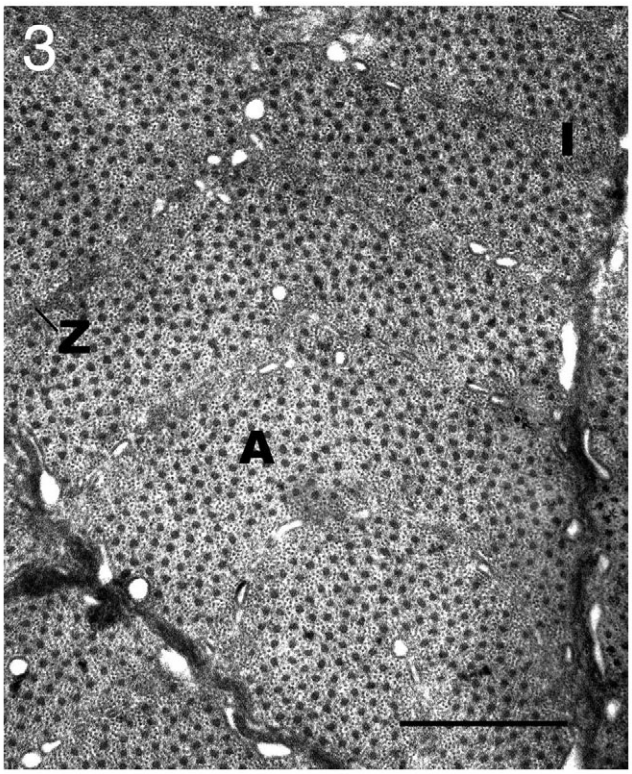

Fig. 3. EM showing ranks of 'myofibrils' oriented approximately perpendicular to the cell surface. Each 'myofibril' is composed of ~8–9 rows of thick filaments with thin filaments interspersed among them, forming the A zone (A), flanked by narrow I zones (I) containing the thin filaments. In some places, radially oriented Z lines (Z) can be seen within the I zones along with cisternae of SR. The latter are also conspicuous along the cell surface. Ferricyanide (black) penetrates into the narrow spaces between the cells but not into the intracellular cisternae. Scale bar, 0.5 μm.

Counts of filaments in the cross-sectioned bundles, extending from one Z region to the next, show a thin/thick ratio of 4.3±0.8. Examination of individual thick filaments typically shows them to be surrounded by coronets of ~8–12 thin filaments (Fig. 5), which are not specifically localized to the trigonal or midpoints between thick filaments.

Longitudinal sections show striations at various angles. As noted previously (Rosenbluth, 1965a), some obliquely striated muscles appear cross striated in one longitudinal plane (Y–Z) and obliquely striated in the perpendicular longitudinal plane (X–Z). Sections at angles between these two show striations at intermediate angles.

In fortuitous sections (Fig. 6), it is possible to follow individual thick filaments from end to end, and in those cases the thick filaments can be seen to measure ~2.8 μm, making them ~75% longer than those of vertebrate striated muscle; i.e. the thick filaments of the squid funnel retractor muscle are both longer and thicker than those of vertebrate skeletal muscle.

Sarcoplasmic reticulum

The typical interface between adjacent muscle fibers consists of the plasma membranes of the respective cells with conspicuous sacs of sarcoplasmic reticulum (SR) on the cytoplasmic side and an intercellular gap that may be only a few hundred angstroms wide. The SR sacs are separated from the sarcolemma by a narrow space

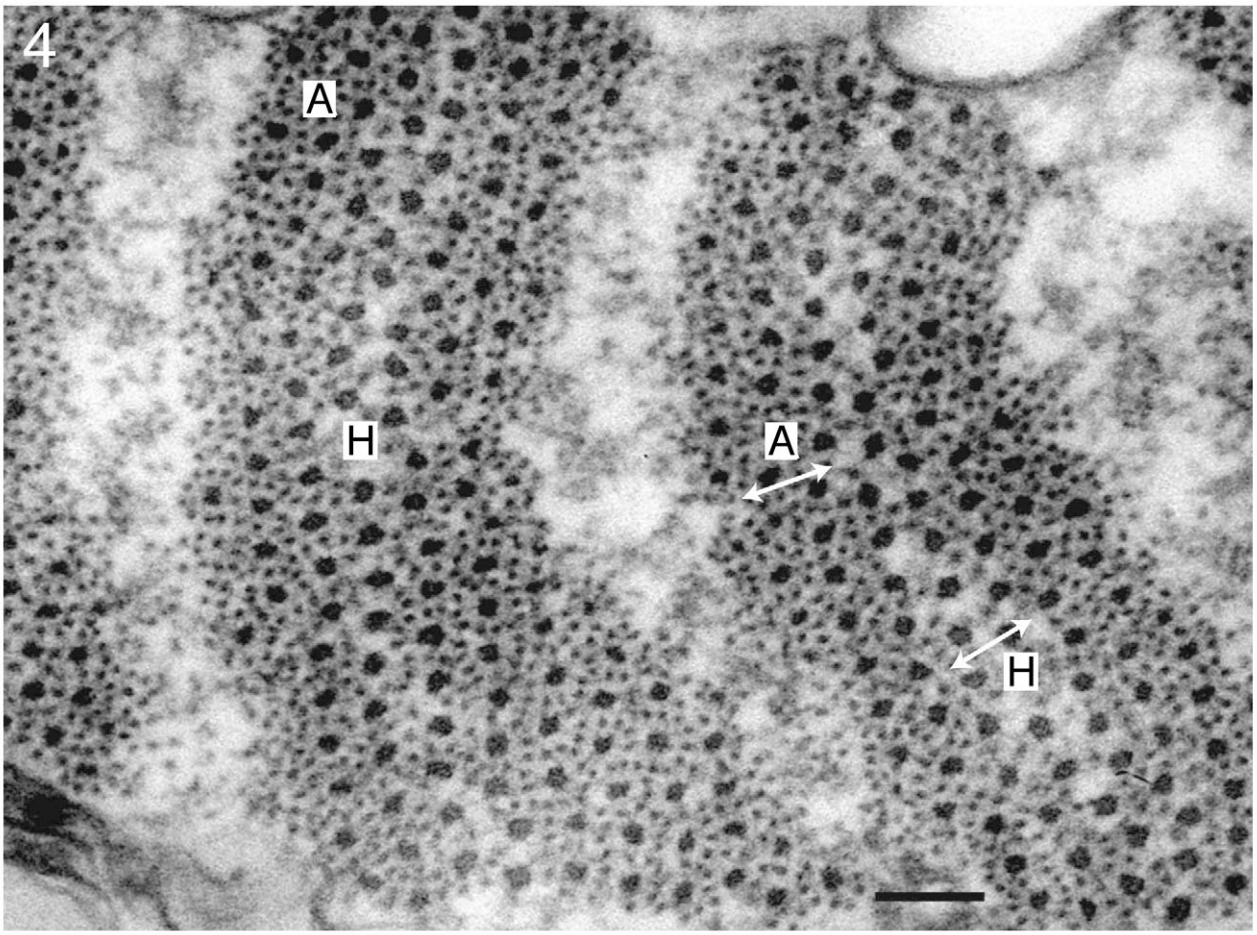

Fig. 4. Myofibers fixed when stretched. The individual 'myofibrils' now consist of only ~five or six rows of thick filaments, i.e. stagger has increased and striation angle has decreased. Thin filaments are absent from the narrow H zone (H, double headed arrow) in the middle of the A zone. Thick filaments in the H zone are clearly thicker than those laterally at the edges of the A zone (A, double headed arrow). Scale bar, 0.1 μm.

containing a moderately dense material, sometimes displaying a periodicity, thus forming dyadic complexes comparable to those of other obliquely striated muscles (Hanson and Lowy, 1961; Rosenbluth, 1968; Rosenbluth, 1969). When two such fibers are apposed, a larger complex may result, consisting of the respective dyads separated by a narrow intercellular gap containing no collagen or other formed elements (Fig. 7).

The appearance of this complex, shown in the diagram in Fig. 8, depends on whether or not ferricyanide, added during tissue processing, has penetrated into the extracellular space. Without ferricyanide, the intercellular gap appears clear, as shown in Fig. 8A. When ferricyanide has penetrated, the intercellular space appears black, as shown in Fig. 8B. In either case, the larger complex, formed by the respective cells, is comparable to that seen

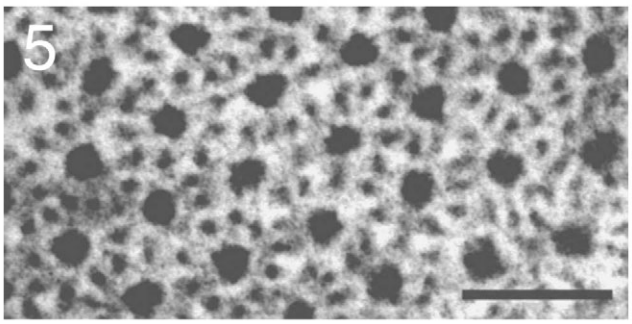

Fig. 5. Detail of A-zone showing a region in which the thick filaments are in hexagonal array. Each is surrounded by 8–12 thin filaments. Scale bar, 0.1 μm.

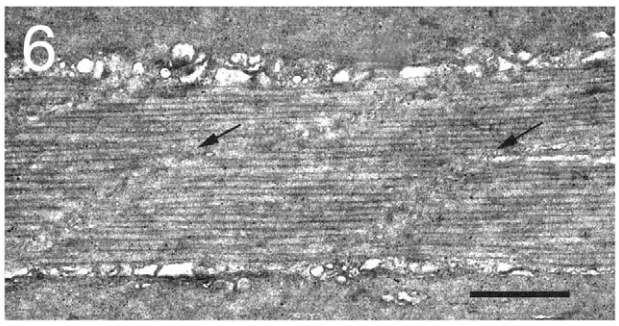

Fig. 6. Longitudinal section of a muscle fiber showing oblique striation. Thick filaments that extend from one I zone to the next (arrows) are ~2.8 μm long. Scale bar, 1 μm.

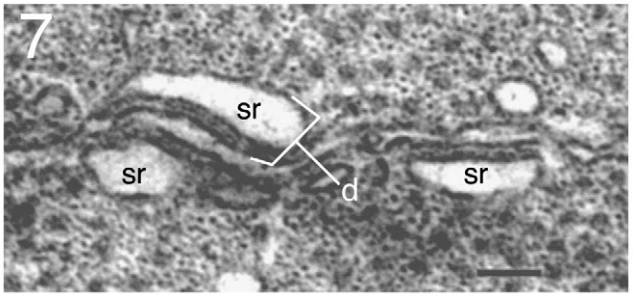

Fig. 7. Confronting dyads in adjacent cells forming a triad-like complex. Each dyad (brackets) consists of an SR cisterna (sr) closely associated with a patch of sarcolemma from which it is separated by a narrow band of moderate density. Scale bar, 0.1 μm.

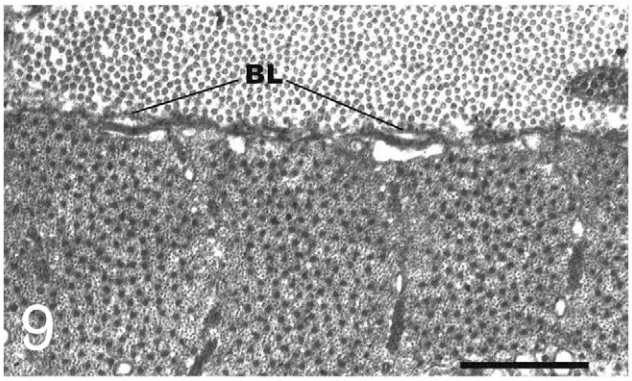

Fig. 9. Muscle cell adjacent to a bundle of collagen fibrils that run parallel to the axis of the myofilaments. The sarcolemma in this region is partially covered by a basal lamina (BL). Scale bar, 0.5 μm.

in the cross-striated muscle of scallop (Nunzi and Franzini-Armstrong, 1981) and closely resembles the 'triad' of vertebrate skeletal muscle (Franzini-Armstrong, 1996), differing in that the central element in vertebrate skeletal muscle is a T-tubule invaginated from the surface rather than an intercellular gap between two separate cells. In both, however, the depolarization that triggers muscle contraction is presumably carried by the membranes of the central element, i.e. the T-tubule in vertebrate skeletal muscle or the apposed plasma membranes in the squid funnel retractor muscle.

Ferricyanide outlines the fibers but does not extend into any intracellular tubular or vesicular structures (Figs 2, 3). Thus, neither the intracellular membranous sacs along the surface nor those extending radially within the I zones are comparable to the T-tubules of skeletal muscle, whose lumina are accessible to extracellular tracers (Huxley, 1964), but, rather, represent a purely intracellular membrane system, the sarcoplasmic reticulum (SR).

In some preparations the contractile apparatus underlying the plasma membrane artifactually shrinks away from it in the apposed cells, but their plasma membranes nevertheless remain closely applied, as if linked together more firmly than the contractile elements to the plasma membrane. Desmosomes interconnecting muscle cells are present in annelid obliquely striated muscles (Rosenbluth, 1968), but no such specialized structural attachments have been seen in the squid funnel retractor muscle. Nor have we seen gap junctions typical of those found in vertebrates, either by transmission electron microscopy or freeze-fracture analysis (data not shown), or evidence of nerve fibers innervating the funnel retractor muscle cells. Although no collagen fibrils or other formed connective tissue elements are visible in the narrow intercellular spaces between squid funnel retractor cells, connective tissue septa composed of tightly packed collagen fibrils, orientated either orthogonal or parallel to the myofilaments are conspicuous in the muscle (Fig. 9). At the interface between a muscle fiber and such a septum, the plasma membrane of the muscle cell does appear to have an indistinct basal lamina (Fig. 9).

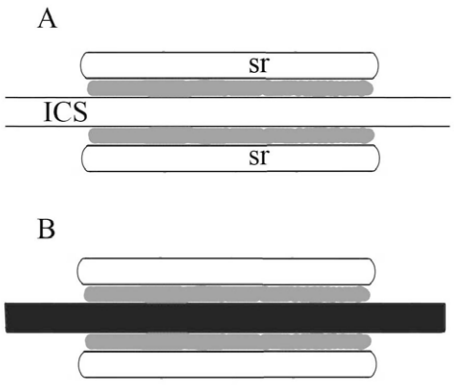

Fig. 8. Diagram showing triad-like complexes formed by adjacent muscle cells separated by the intercellular space. (A) Each cell has a sac of sarcoplasmic reticulum (sr) apposed to the cytoplasmic surface of the cell. A moderately dense material, shown in gray, intervenes between the sr sac and the plasma membrane. The intercellular space (ICS) is clear. (B) Same as A, except that in this case the ICS is filled with ferricyanide and appears black.

Contractile properties

The mean (±s.d.) peak isometric stress (P_0) of the preparations in tetanus (150 Hz, 2 ms pulses, 200 ms duration) was 270±20 mN mm^2 physiological cross section. The mean twitch:tetanus ratio was 0.11±0.043. Brief tetanic stimulations less than 60 Hz did not result in fusion (Fig. 10A,B). The mean latent period (T_L) for both twitch and brief tetanus was 8±1.1 ms (Fig. 10A). The mean time to peak force (T_P) was 50±4.3 ms for twitch and 120 ±18 ms for brief tetanus (Fig. 10A).

The maximum unloaded shortening velocity (V_{max}) of the funnel retractor muscle preparations was 2.15±0.26 L_0 s^{-1} (mean ± s.d.), where L_0 was the preparation length that generated peak force in brief tetanus (Fig. 10C). The peak power output of the funnel retractor muscle preparations was 37.6±13.7 W kg^{-1} (mean ± s.d.). About 20% (data not shown) of the cross-sectional area of the muscle preparations was occupied by the remains of the severed transverse muscle fibers. Furthermore, the core of mitochondria occupied a mean of 10.6% of the cross-sectional area of a single longitudinal fiber (data not shown). Correcting the peak power output for these components that did not contribute force to the preparation yielded a mean peak power output of 49.9 W kg^{-1} (Fig. 10D). The relative power output (i.e. $V/V_{max} \times P/P_0$) of the funnel retractor muscle preparations was 0.16±0.041 (Fig. 10D). The funnel retractor muscle preparations generated peak power at a V/V_{max} of 0.33±0.044 (Fig. 10D).

In vivo muscle length changes

Our *in vitro* physiology data showed that the longitudinal fibers of the funnel retractor muscle are activated and generate force rapidly, but their low V_{max} and the short duration of a single jet pulse led us

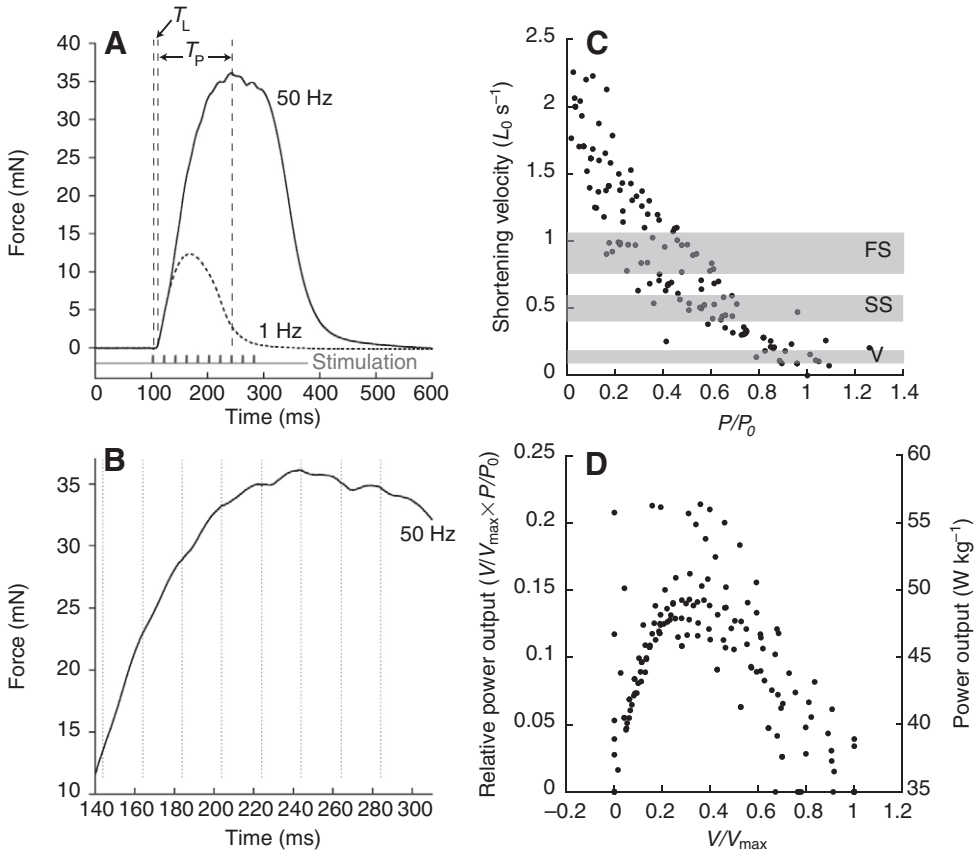

Fig. 10. Contractile properties of the longitudinal fibers. (A) Time course of force production in the longitudinal muscle fiber preparations during twitch (dotted line) and brief tetanic (50 Hz, solid line) stimuli. The timing of the tetanic stimuli are indicated in gray beneath the force traces; the timing of the single twitch stimulus coincides with the first tetanic stimulation. The latent period (T_L, i.e. the time between the start of the first stimulus and the start of force rise) and the time to peak (T_P, i.e. the time from the first rise in force to the peak) are also indicated. (B) An expanded view of the peak of the brief tetanic force trace to illustrate the effect of individual stimuli. The vertical dashed lines indicate the timing of stimuli. (C) Force–velocity relationship and (D) power output of the longitudinal muscle fiber preparations stimulated in brief tetanus (50 Hz, 2 ms pulses, 200 ms duration). The gray boxes in C show the mean range of *in vivo* strain rate (see Fig. 13B) of the funnel retractor muscle during the exhalant phase of ventilatory jets (V; animal was stationary), slow swimming (SS; <1 DML s^{-1}), and fast swimming (FS; >3 DML s^{-1}). C and D contain data from 10 preparations.

to hypothesize that the whole muscle experiences low shortening strain *in vivo*. Although this prediction did not stem from the consideration of the biochemistry of funnel retractor muscle myosin that was the prime motivation of this study, we nevertheless saw an opportunity to test this intriguing hypothesis using sonomicrometry.

The muscle shortened and elongated rhythmically during locomotion and ventilation of the mantle cavity (Fig. 11). During the low amplitude contractions, and subsequent expansions, of the mantle used to ventilate the mantle cavity, the onset of shortening of the funnel retractor muscle and the onset of mantle contraction at the start of the exhalant phase of ventilation were nearly out of phase (Fig. 11B). If a single exhalant–inhalant jet cycle is composed of 360 deg and the start of mantle contraction during the exhalant phase begins at 0 deg, the onset of funnel retractor muscle shortening occurred at –131±35.5 deg (mean ± s.d.; Fig. 12). As the speed of swimming increased, the onset of funnel retractor muscle shortening nearly coincided with the start of mantle contraction for both arms-first and tail-first swimming (Fig. 11A). The phase of the onset of funnel retractor muscle shortening was –32.3±19.4 deg, –56.5±24.9 deg, –21.8±15.5 deg and –23.8 ±16.5 deg for tail-first and arms-first slow swimming, and for tail-first and arms-first fast swimming, respectively (Fig. 12).

The funnel retractor muscle experienced low strains during ventilation of the mantle cavity and locomotion (Fig. 11 and Fig. 13A). During ventilation, the funnel retractor muscle elongated during the exhalant phase of the jet and the total range of strain was ±0.025±0.013 (±s.d.). The muscle shortened during the exhalant phase of slow and fast swimming, and the maximum shortening strain was always greater than the elongation strain (Fig. 13A). The total range of strains was 0.039±0.028 to –0.067±0.029 and 0.029±0.028 to –0.061±0.021 for tail-first and arms-first slow swimming, respectively, whereas for tail-first and arms-first fast swimming, the total range of strains was 0.07±0.034 to –0.13±0.025 and 0.075±0.03 to –0.15±0.04, respectively (Fig. 13A).

During the exhalant phase of the jet, the range of strains experienced by the funnel retractor muscle was lower, with a mean range of less than ±0.04 for ventilation, tail-first slow and fast swimming, and arms-first slow and fast swimming (Fig. 13A). For most of the arms-first slow jets, the muscle was virtually isometric during the exhalant phase of the jet (Fig. 13A; see example in Fig. 11).

The shortening and elongation velocities of the funnel retractor muscle were low during ventilation and, with the exception of arms-first slow swimming, increased with swimming speed (Fig. 13B). The mean shortening velocity was 0.16±0.064 L_R s^{-1} (where L_R was the resting length of the funnel retractor muscle) during ventilation, 0.51±0.21 L_R s^{-1} and 0.25±0.053 L_R s^{-1} during tail-first and arms-first slow swimming, respectively, and 0.91±0.24 L_R s^{-1} and 0.76±0.17 L_R s^{-1} during tail-first and arms-first fast swimming, respectively.

DISCUSSION

Our principal findings on the longitudinal fibers of the funnel retractor muscles are as follows. (1) The funnel retractor muscle consists of small, spindle-shaped fibers that have a double array of myofilaments in an obliquely striated organization with abundant sarcoplasmic reticulum and minimal intercellular connective tissue elements. (2) The activation of the longitudinal fibers is rapid and comparable to that of the cross-striated scallop adductor muscle. (3) The longitudinal fibers have a low V_{max} and generate a modest amount of power. (4) The muscle operates *in vivo* over a narrow range of lengths (±4% of resting length) during most jets. (5) The fibers are not individually innervated. In that

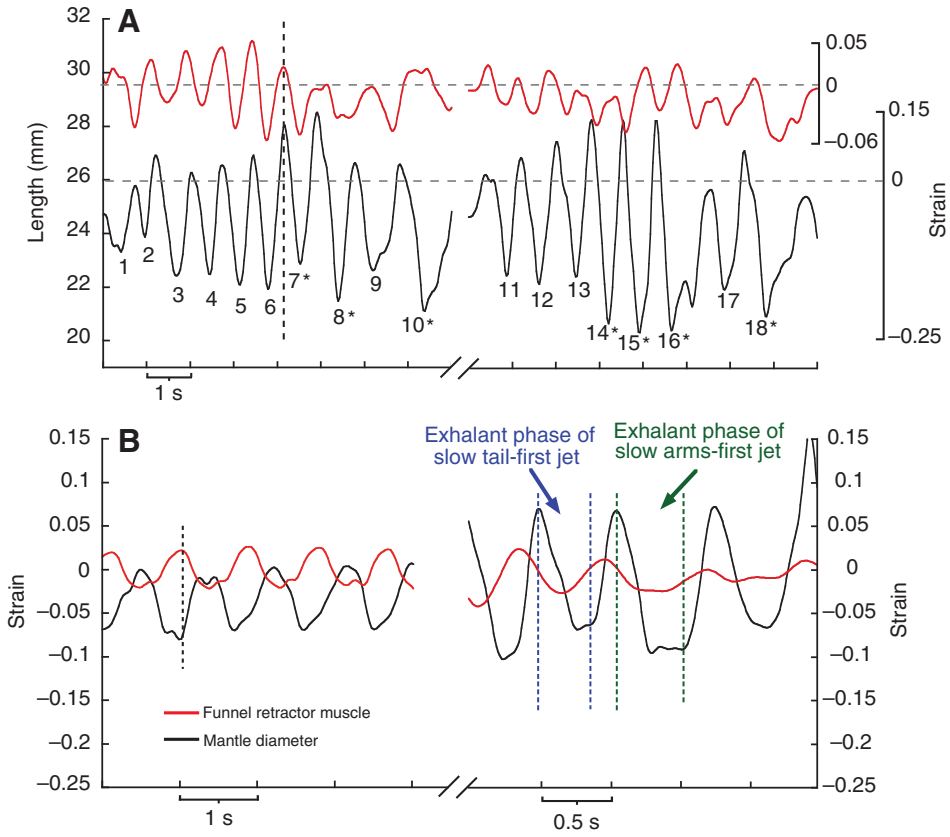

Fig. 11. Variation in the length and longitudinal strain of the funnel retractor muscle (red) and in the diameter and circumferential strain of the mantle (black) during ventilatory movements of the mantle and also during slow (<1 DML s^{-1}) and fast (>3 DML s^{-1}) swimming. Negative strain indicates shortening (i.e. decrease in diameter of the mantle and decrease in length of the funnel retractor muscle). (A) A series of 18 slow and fast (*) tail-first jets. The vertical dashed line helps show that the onset of funnel retractor shortening nearly coincides with the start of mantle contraction during fast jets. (B) Ventilatory movements (left side) and slow jets (right side). During ventilation, note the low strain experienced by the funnel retractor muscle and that maximum funnel retractor muscle shortening is almost completely out of phase with the maximum mantle contraction (dashed vertical line). During slow swimming, the blue dotted lines indicate the exhalant phase (i.e. ejection of water from the mantle) of one tail-first jet, and the green dotted lines indicate the exhalant phase of the arms-first jet. During the tail-first jet, the funnel retractor muscle shortens slightly during mantle contraction but then begins elongation just prior to the start of the inhalant phase of the jet. During the arms-first jet, the funnel retractor also shortens slightly but then remains nearly isometric throughout most of the exhalant phase. Note the different time scales during slow swimming and ventilation.

respect the funnel retractor muscle resembles a 'unitary' smooth muscle.

The funnel retractor muscle is composed of obliquely striated fibers

Our principal morphological finding is that the longitudinal fibers of the funnel retractor muscle, which were previously thought to be 'smooth', are in fact obliquely striated; i.e. the tips of the thick filaments align to form a very small angle with respect to the filament axis instead of 90 deg, as in cross-striated muscles. Shortening of this type of muscle has been shown to entail not only the sliding of thin filaments with respect to thick (Hanson and Lowy, 1964; Rosenbluth, 1965a; Rosenbluth, 1968) but also 'shearing' of thick filaments with respect to one another (Rosenbluth, 1965a), resulting in a change in striation angle. This architectural arrangement may have an important consequence, as discussed below, in that friction associated with myofilament shearing could account for some of the physiological properties of this kind of muscle, compared with those of cross-striated muscles, such as the scallop adductor, which do not exhibit shearing.

The funnel retractor muscle is activated rapidly

The physiological data support the prediction that the longitudinal fibers of the funnel retractor muscle are activated and produce force rapidly. The latent period (T_L) between electrical stimulus and the rise of force during isometric contraction is comparable to that of the obliquely striated circular muscles of the mantle [which also have abundant sarcoplasmic reticulum (Thompson et al., 2008)] of *D. pealeii* at 20°C, and only slightly shorter than the T_L of the striated adductor muscles of *A. irradians* at 15°C (13.95 ms) and 20°C (10.42 ms) (Olson and Marsh, 1993). In addition, the high fusion frequency of the fibers (Fig. 10B) relative to the obliquely striated mantle muscles of squid (see Milligan et al., 1997) suggests rapid activation and deactivation (see Marsh, 1990; Askew and Marsh, 1998). Finally, the time to peak force (T_P) for a twitch, 50 ms in the longitudinal fibers of the funnel retractor muscle, is shorter than the twitch T_P (62.35 ms) for the striated adductor of *A. irradians* at 20°C and both the obliquely striated central mitochondria poor (143 ms) and superficial mitochondria rich (143 ms) circular muscle fibers of the mantle of *D. pealeii* at 20°C (Thompson et al., 2008). Indeed, it is comparable to the T_P of two fast-acting vertebrate fibers: the fast glycolytic iliofibularis muscle of the lizard *Dipsosaurus dorsalis* (~50 ms) (Marsh and Bennet, 1985) and the gastrocnemius of the leopard frog *Rana pipiens* (48 ms) (Osgood and Brewster, 1963) at 20°C. Although the T_P of the longitudinal fibers of the funnel retractor muscle is quite low, it nevertheless does not approach the extremely short T_P of muscles specialized for exceptionally rapid activation and force production [e.g. 3 ms at 17°C in 'remotor' muscle of the lobster *Homarus americanus* (Mendelson, 1969); <6.6 ms at 30°C in the singing muscle of the cicada *Psaltoda claripennis* (Young and Josephson, 1983)], even when allowances are made for the different temperatures at which the experiments were conducted.

The rapid activation and force rise of the longitudinal fibers in the funnel retractor muscle is correlated with abundant SR, thus supporting our prediction. The abundance of SR in fast-acting muscles has been well established in cross-striated muscles of both vertebrates (Fawcett and Revel, 1961) and invertebrates (Rosenbluth, 1969). This generalization applies to obliquely striated muscle as well; i.e. the slow muscles of nematodes display relatively little SR (Rosenbluth, 1969) in contrast to fast-acting annelid muscles, whose fibers have dyads over much of their surface (Rosenbluth, 1968; Knapp and Mill, 1971). SR in the squid funnel retractor muscle

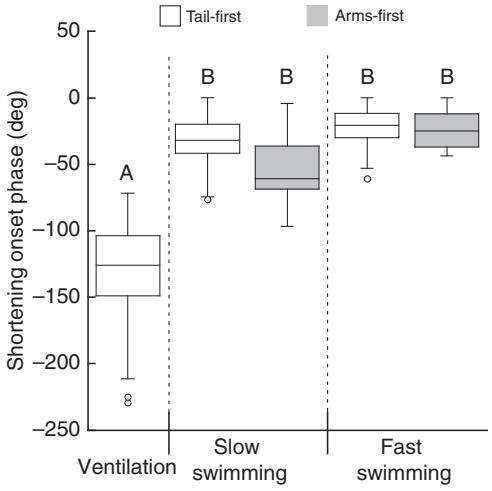

Fig. 12. The relative timing of shortening of the funnel retractor muscle and decrease in mantle diameter during ventilatory movements of the mantle, slow swimming (<1 DML s^{-1}), and fast swimming (>3 DML s^{-1}). The onset of shortening by the funnel retractor muscle began prior to the onset of the exhalant phase for all jets. For ventilatory mantle movements, the funnel retractor and mantle were nearly out of phase, but were nearly in phase during swimming. This suggests that the timing of funnel retractor muscle activation may differ between ventilation and swimming, and may indicate that the muscle serves different functions during these behaviors. The letters indicate statistical differences: A *vs* B, one-way ANOVA, $P<0.001$; B *vs* B, $P>0.95$. For this, and the boxplots in Fig. 13, the line in each box indicates the mean, the upper and lower limits of the box indicate the upper and lower quartiles, and the whiskers show the 95% confidence intervals. Outliers (circles) represent values outside the confidence intervals. Sample size: 20 jets of each type per squid; total, four squid.

is also abundant, covering much of the surface of the fibers and extending radially inward in the I zones as well. Thus, with respect to its complement of SR, the squid funnel retractor muscle is similar to that in other fast-acting obliquely striated muscles and different from the slow nematode muscle.

The relatively high fusion frequency of the funnel retractor muscle of *D. pealeii* was intriguing given the low twitch:tetanus ratio. By comparison, experiments on whole (i.e. both transverse and longitudinal fibers were intact) funnel retractor muscles in *Octopus vulgaris* and the European cuttlefish *Sepia officinalis* had similar twitch:tetanus ratios but their fusion frequencies were only 20 Hz and 50 Hz, respectively (Lowy and Millman, 1962). The differences in fusion frequencies may be related to differences in the rates of Ca^{2+} flux across the sarcoplasmic reticulum, but further investigation is needed to determine the cause. A common feature of all the preparations was that at 50 Hz stimulation (2 ms pulses, 200 ms duration) force began to decline following the eighth stimulus (in the train of 10 stimuli; see Fig. 10A,B), suggesting that the balance of Ca^{2+} flux across the sarcoplasmic reticulum shifted toward uptake. This phenomenon was not observed at stimulation frequencies greater than 60 Hz, in which force did not fall until after the final stimulus in the train.

Funnel retractor muscle fibers do not shorten rapidly

Given the short T_P of the funnel retractor muscle and the inverse relationship between T_P and maximum unloaded shortening velocity (Close, 1965), we predicted that the longitudinal fibers of the funnel retractor muscle would exhibit high maximum unloaded shortening velocity (V_{max}). We found no support for this prediction. The V_{max} of the funnel retractor muscle of *D. pealeii* was relatively low. It was similar to that of the superficial mitochondria rich (SMR) circular muscle fibers ($2.1\,L_0\,s^{-1}$ at 20°C) (Thompson et al., 2008) of the mantle of *D. pealeii*, and also was in the range of measured values ($0.6–3.0\,L\,s^{-1}$) for the striated adductor muscles of the scallop *Pecten* sp. at 14°C (Abbot and Lowy, 1957). However, it was considerably lower than the V_{max} of the striated adductor of *A. irradians*. Given the Q_{10} of 2.41 over the temperature range of 15–20°C reported by Olson and Marsh (Olson and Marsh, 1993), the V_{max} of *A. irradians* cross-striated muscle at 17°C, the temperature at which we conducted our experiments, would be about $7.8\,L_0\,s^{-1}$. This is 3.6 times higher than the V_{max} value we measured for the longitudinal fibers of the funnel retractor muscle.

The thick filaments of the longitudinal fibers of the funnel retractor muscle are longer than those of the striated adductor (2.8 μm *vs* 1.7 μm) (Morrison and Odense, 1968; Millman and Bennett, 1976). If extensive (*sensu* Josephson, 1975) regulation of shortening velocity alone occurred in scallops and squids, the shorter thick filaments of *A. irradians* and *P. magellanicus* would have resulted in a 1.6-fold higher V_{max} for the scallop muscle (all else equal), instead of the 3.6-fold difference we report. Despite the similarities in ATPase activity of the myosin S1 fragments between squid and scallops, therefore, other aspects of the fibers or myosins (e.g. light chains, duty cycle) must differ. In this context, we suggest that oblique striation may impose constraints on shortening velocity because the friction associated with shearing of the thick filaments (see Rosenbluth, 1965a; Rosenbluth, 1968) may act as a brake. Thick filament shearing does not occur in cross striated muscles, including the striated scallop adductors.

Power output

The peak power (49.9 W kg^{-1}; Fig. 10D) of the funnel retractor muscle is less than half the peak power output measured using work loop techniques for the striated adductor of the scallop *A. irradians* at 10°C (Marsh and Olson, 1994). Relative to other cross-striated muscles, the power output (in W kg^{-1}) of the longitudinal fibers is similar to that of the red fibers of carp (Rome and Sosnicki, 1990) and scup (Rome et al., 1992) at 10°C, and the FG portion of the iliofibularis of the lizard *Dipsosaurus dorsalis* at 15°C (Marsh and Bennett, 1985). The power output is quite low, however, relative to the fast-acting fibers of *Xenopus laevis* iliofibularis muscle at 20°C (Lännergren, 1987) and the flight muscles of katydids at 35°C (Josephson, 1984), even after accounting for differences in temperature. Although the peak power output of the longitudinal fibers of the funnel retractor muscle is comparable to that of one fast-acting muscle, in general it is low relative to others. Friction associated with shearing of the thick filaments may constrain not only shortening velocity but also peak power output.

In vivo function of the funnel retractor muscle

Our *in vitro* physiology data show that the longitudinal fibers of the funnel retractor muscle are activated and generate force rapidly, but their low V_{max} and the short duration of a single jet pulse led us to hypothesize that the whole muscle experiences low shortening strain *in vivo*. The sonomicrometry data support this hypothesis. During ventilation and swimming, the funnel retractor muscles experience low strains, particularly during the exhalant phase of the jet (Fig. 13A). The funnel retractor muscles experienced a range of strains during the exhalant phase of less than ±0.04 for fast swimming but less than ±0.025 for ventilation and slow swimming (Fig. 13A). For many bouts of arms-first slow swimming and all

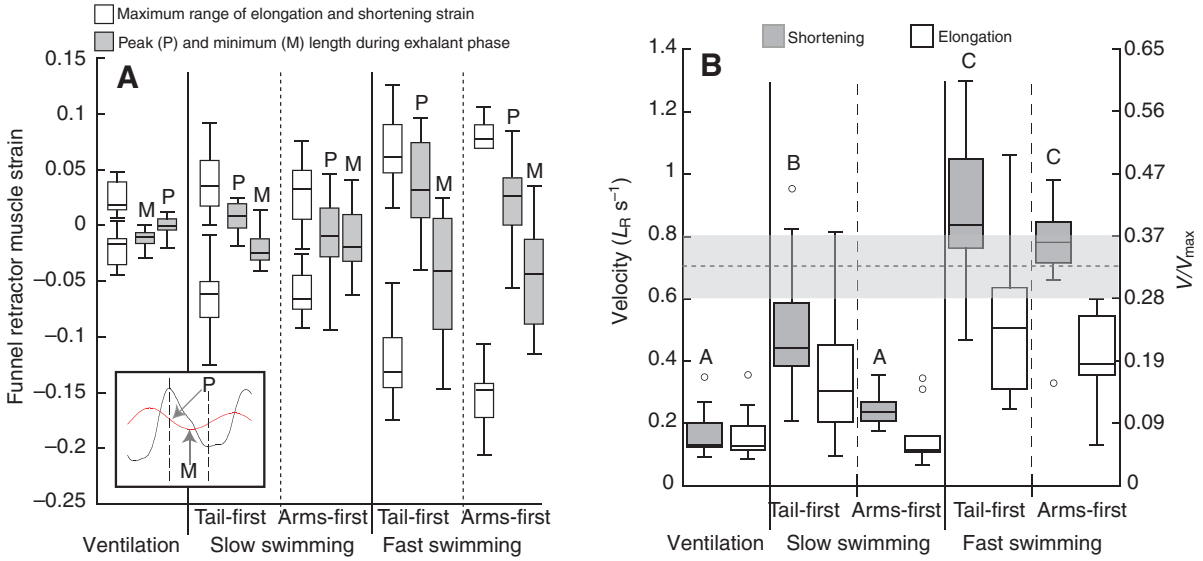

Fig. 13. (A) Funnel retractor muscle strain during mantle cavity ventilation and slow (<1 DML s^{-1}) and fast (>3 DML s^{-1}) swimming. In each category, the two white boxes represent the maximum elongation and shortening strains of the funnel retractor muscle during one jetting cycle (i.e. the full range of funnel retractor muscle length change during a single jet cycle). The two gray boxes represent the peak and minimum funnel retractor length (relative to resting length, i.e. strain) only during the exhalant phase of the jet (see inset). The funnel retractor muscle elongates slightly during ventilation but shortens during slow and fast swimming. The maximum amplitude of funnel retractor shortening increases as the amplitude of mantle contraction increases but the mean strain during the exhalant phase remains within ±0.04 for all swimming speeds. The funnel retractor muscle strains at the start and end of the exhalant phase of the jet were not significantly different from each other for ventilation (P=0.76) and tail-first (P=0.15) or arms-first (P=0.99) slow swimming, but were significantly different for both tail-first and arms-first fast swimming (P<0.001 for both comparisons; one-way ANOVA with Tukey's highly significant post test; sample size: 20 jets of each type per squid; total, four squid). (B) Velocities of shortening and lengthening of the funnel retractor muscle during mantle cavity ventilation and jetting. Velocity is reported relative to the 'resting' length (L_R) of the funnel retractor muscle and also relative (V/V_{max}) to the maximum unloaded shortening velocity of the longitudinal fiber preparations measured *in vitro*. The gray shaded region encompasses the mean ± s.d. (0.33±0.044) V/V_{max} at which the longitudinal fiber preparations produced peak relative power; the horizontal dotted line indicates the mean. The letters indicate statistical differences between shortening velocities: A *vs* A, P>0.53; A *vs* B, P<0.001; A *vs* C, P<0.0001; one-way ANOVA with Tukey's highly significant post test; sample size: 20 jets of each type per squid; total, four squid.

ventilatory jets, the muscle was virtually isometric during the exhalant phase of the jet (see example in Fig. 11B).

Although it experienced low strains, the funnel retractor muscle did shorten by more than 15% of its resting length during the exhalant phases of some fast tail-first and arms-first jets. The functional significance of these higher strains is not clear, although movements of the funnel retractor muscle and subsequent protrusion or retraction of the funnel may have fluid dynamic consequences for the propulsive efficiency or thrust of the pulsed jet (see Anderson and Grosenbaugh, 2005; Bartol et al., 2008; Bartol et al., 2009).

Given the low strain experienced by the funnel retractor muscles and the ability of the longitudinal fibers to produce relatively high peak isometric stress, the role of the funnel retractor muscles may be to stabilize the base of the funnel, at least during ventilation and slow jets, i.e. the funnel retractor muscles may act as muscular struts. Muscular struts (see Dickinson et al., 2000) have been reported to stabilize the joints of animals with rigid skeletal support systems during locomotion (Roberts et al., 1997; Fukunaga et al., 2001) or transmit forces generated by adjacent myomeres (Wardle et al., 1995; Shadwick et al., 1998; Gillis, 1998; Altringham and Ellerby, 1999). Many of these muscles produce force isometrically during one phase of locomotion (e.g. the stance phase of walking or hopping) (Roberts et al., 1997; Biewener et al., 1998; Fukunaga et al., 2001) but may shorten or elongate considerably during other phases of the locomotory cycle.

The limited length operating range of the funnel retractor muscles, especially during ventilation and slow jetting, is consistent with the characteristics of a muscular strut. We plan to measure EMG activity in the longitudinal fibers during locomotion to test this hypothesis of funnel retractor muscle function.

Structural correlates of funnel retractor muscle function

The contractile elements of cross-striated muscles are linked together in series so that the forces generated are transmitted to tendons at the ends, and synchronous contraction of the chain of sarcomeres results in extensive, rapid shortening. The contractile elements of smooth muscles, by contrast, are attached in parallel to extracellular connective tissue elements along the sides of the fibers, resulting in slow contraction but with amplification of the forces such that even smooth muscles containing relatively little myosin can generate significant force (Rosenbluth, 1965b). Obliquely striated muscles occupy an intermediate position and may be adapted to function in either of these two ways.

The obliquely striated squid funnel retractor muscle is unusual in that it shows no evidence of either attachments linking its longitudinal muscle cells together in series or of connections between the contractile elements and the extracellular matrix along the sides that would link the fibers in parallel. Thus, in this case the mechanisms that transmit the stresses of muscle fiber contraction are unclear. This apparent absence of force-transmitting structures suggests that the funnel retractor muscle may not function to shorten extensively or to generate large tensions but rather to simply stiffen into a semi-rigid structural element. Our rationale is as follows.

In the slow obliquely striated body musculature of the nematode worm *Ascaris lumbricoides* (Rosenbluth, 1965a), dense bodies, into which thin filaments insert, are conspicuous all along the sides of

the muscle fibers, where they associate closely with the connective tissue elements that are so abundant between adjacent fibers. Thus, it is likely that the forces developed by contractile elements within each fiber are to some extent exerted in parallel, and are thus additive.

The fast obliquely striated muscle of the annelid worm *Glycera dibranchiata*, by contrast, shows no attachment of contractile elements to endomysium along the sides of the fibers. Indeed, the *G. dibranchiata* muscle is virtually devoid of endomysium. It does, however, display conspicuous desmosomal cell-to-cell attachments, consistent with cells linked to one another in series. Thus the *G. dibranchiata* muscle appears to be adapted to shortening rather than to magnifying the forces generated by exerting them in parallel. These structural differences correlate very well with the slow forcible movements of *A. lumbricoides* and the rapid contractions displayed by *G. dibranchiata*.

The squid funnel retractor muscle resembles the *G. dibranchiata* muscle in that its component fibers are not separated from one another by endomysium, and there is no evidence of attachment of the contractile apparatus along the sides of the fibers. Its conformation therefore appears not to be adapted to addition of forces acting in parallel. Indeed, the peak force generated by the funnel retractor muscle (270 mN mm^{-2}) is only moderately greater than the ~100–200 mN mm^{-2} produced by the cross-striated scallop adductor (Marsh and Olson, 1994), a difference that can easily be accounted for by the difference in thick myofilament length [~2.8 μm in the squid funnel retractor muscle *vs* ~1.7 μm in the scallop adductor (Morrison and Odense, 1968; Millman and Bennett, 1976; Vibert and Castellani, 1989)].

However, the squid funnel retractor muscle shows no evidence of desmosomal attachments between muscle cells, like those seen in *Glycera* muscle and those linking scallop adductor muscle fibers together in series (Nunzi and Franzini-Armstrong, 1981). Thus, the structure of the funnel retractor muscle provides no evidence that it is adapted either to the generation of large forces or to extensive shortening. Based on its structural organization we propose, therefore, that contraction of the funnel retractor muscle results primarily in near isometric stiffening of the muscle into a strut, requiring neither extensive shortening nor force amplification.

How are the longitudinal fibers activated?

Young (Young, 1938) reported that two giant axons, via branches of the visceral nerve, and several smaller nerves innervate each funnel retractor muscle. In addition, Young was able to distinguish the force responses of the two giant axons, which differed in diameter, by varying the stimulatory voltage. Furthermore, he elicited small graded force responses from the funnel retractor muscle, which he interpreted as evidence of stimulation of small motor axons (Young, 1938). Thus, we were surprised by the apparent absence of motor axons in the funnel retractor muscle.

The lack of an abundant innervation of the funnel retractor muscle may imply that its fibers are electrically interconnected, as are the 'unitary' smooth muscles of vertebrates, rather than individually innervated. However, we have seen no evidence of gap junctions between adjacent muscle fibers. Failure to identify such structures in the funnel retractor muscle could reflect structural differences in electrically coupled junctions of cephalopods or simply disjunction during processing of the tissues. Alternatively, since the muscle cells are very closely apposed, they may be activated by field potentials, which would have the virtue of synchronizing rapid activation of the funnel retractor muscle such that the individual fibers of the funnel retractor would act more or less in unison as if they were in fact a single large fiber.

Does myosin-linked regulation confer specific contractile properties on a muscle?

Force production by the funnel retractor muscle of *D. pealeii* and the striated adductors of *P. magellanicus* and *A. irradians* is controlled by remarkably similar regulatory systems (Lehman and Szent-Györgyi, 1975; Simmons and Szent-Györgyi, 1980; Perreault-Micale et al., 1996; Kalabokis and Szent-Györgyi, 1997; Yang et al., 2007) (L. O'Neall-Hennesey, personal communication). Our data show that the longitudinal fibers of the funnel retractor muscle, like the striated adductors, are activated rapidly and generate force rapidly during a twitch. Thus, myosin-linked regulation is correlated with rapid activation and force production.

Despite similarities in activation kinetics, the V_{max} and P_0 of the scallop and squid muscles differ considerably, and identifying the cause of this discrepancy is important to understanding how myosin-linked regulation affects contractile properties. Simmons and Szent-Györgyi (Simmons and Szent-Györgyi, 1978; Simmons and Szent-Györgyi, 1980) have shown that fiber bundles of *P. magellanicus* can be obtained at low ionic strength by chemical skinning. These muscle fibers retain their relative positions and their filamentous structures. The regulatory light chain present associated with the myosin can be removed by EDTA treatment at room temperature and the resulting muscle develops rigor and loses its ability to bind Ca^{2+}. Ca^{2+} can be rebound by the re-addition of pure regulatory light chain, thereby restoring regulation and indicating that the regulatory light chain acts as a regulatory switch (Simmons and Szent-Györgyi, 1978). Interestingly, foreign regulatory light chains from the adductors of bivalves (*Spisula* spp. and *Mercenaria mercenaria*) and the funnel retractor muscle of *D. pealeii* also restore regulation. Moreover, the regulatory light chain from chicken gizzard, which requires phosphorylation for regulation, also restores regulation to the chemically skinned fibers of *P. magellanicus* (Simmons and Szent-Györgyi, 1980). Regulatory light chains from fast fibers in the abdomen of lobster (*Homarus americanus*), bovine cardiac muscle and rabbit striated muscles were unable to restore regulation (Simmons and Szent-Györgyi, 1980) (for details, see Simmons and Szent-Györgyi, 1985). These experiments suggest that the unexpected low V_{max} and high P_0 of the funnel retractor fibers relative to the scallop striated adductor result from events occurring later than the regulatory process. We therefore attribute these differences in the squid and scallop muscles to the arrangement of the myofilaments (oblique *vs* cross striation) and also to the longer thick filaments of the funnel retractor muscle.

Concluding remarks

We describe the ultrastructure and contractile properties of the funnel retractor muscle of *D. pealeii* as part of a comparative study of myosin-regulated muscles. Our data show that, like the myosin-regulated striated adductor of *A. irradians* and *P. magellanicus*, the funnel retractor muscle is activated rapidly and generates force rapidly. Its low V_{max} in combination with the relatively short time course of a jet lead to a limited length operating range for the funnel retractor muscles *in vivo*, consistent with our proposal that it acts primarily as a strut during ventilation and slow swimming.

LIST OF ABBREVIATIONS

DML	dorsal mantle length
G	the constant expressing curvature of the force–velocity relationship (see Hill, 1938)
L_0	muscle preparation length that generated the maximum isometric stress
L_I	instantaneous distance between the sonomicrometry transducers

L_R	distance between the sonomicrometry transducers with the funnel retractor muscle at rest
P_0	peak isometric stress in tetanus
P^*	the intercept on the force axis for the hyperbolic curve-fitting to the force-velocity data
T_L	latent period; time from the start of the first stimulus to the onset of force rise
T_P	time to peak force; time from the onset of force rise to peak force
V_{max}	maximum unloaded shortening velocity measured *in vitro*
V/V_{max}	*in vivo* muscle shortening velocity relative to V_{max}

ACKNOWLEDGEMENTS

We thank Steven Jarzembowski, and Kari Taylor for help with the muscle mechanics experiments, and Dr Kevin Eckelbarger, Timothy Miller and Linda Healy at the Darling Marine Center for providing housing, laboratory space and aquaria for the squid. We thank Chris Petzold (NYUMC) for expert technical assistance. Financial support was provided to J.R. by NIH grant NS037475, to A.G.S. by NIH grant AR017346 to Dr Carolyn Cohen (Brandeis University), and to J.T.T. by NSF grant IOS-0446081 and Franklin & Marshall College (start-up funding, Hackman Summer Fellowship Program, and the Committee on Grants). Deposited in PMC for release after 12 months.

REFERENCES

Abbott, B. C. and Lowy, J. (1957). Stress relaxation in muscle. *Proc. R. Soc. Lond. B. Biol. Sci.* **146**, 281-288.
Altringham, J. D. and Ellerby, D. J. (1999). Fish swimming: patterns in muscle function. *J. Exp. Biol.* **202**, 3397-3403.
Anderson, E. J. and Grosenbaugh, M. A. (2005). Jet flow in steadily swimming adult squid. *J. Exp. Biol.* **208**, 1125-1146.
Askew, G. N. and Marsh, R. L. (1998). Optimal shortening velocity (V/V_{max}) of skeletal muscle during cyclical contractions: length-force effects and velocity-dependent activation and deactivation. *J. Exp. Biol.* **201**, 1527-1540.
Bárány, M. (1967). ATPase activity of myosin correlated with speed of muscle shortening. *J. Gen. Physiol.* **50**, 197-218.
Bartol, I. K., Krueger, P. S., Thompson, J. T. and Stewart, W. J. (2008). Swimming dynamics and propulsive efficiency of squids throughout ontogeny. *Int. Comp. Biol.* **48**, 720-733.
Bartol, I. K., Krueger, P. S., Stewart, W. J. and Thompson, J. T. (2009). Hydrodynamics of pulsed jetting in juvenile and adult brief squid *Lolliguncula brevis*: evidence of multiple jet 'modes' and their implications for propulsive efficiency. *J. Exp. Biol.* **212**, 1889-1903.
Biewener, A. A., Konieczynski, D. D. and Baudinette, R. V. (1998). *In vivo* muscle force-length behavior during steady-speed hopping in tammar wallabies. *J. Exp. Biol.* **201**, 1681-1694.
Bower, J. R., Sakurai, Y., Yamamoto, J. and Ishii, H. (1999). Transport of the ommastrephid squid *Todarodes pacificus* under cold-water anesthesia. *Aquaculture* **170**, 127-130.
Close, R. (1965). The relation between intrinsic speed of shortening and duration of the active state of muscle. *J. Physiol.* **180**, 542-559.
Dickinson, M. H., Farley, C. T., Full, R. J., Koehl, M. A. R., Kram, R. and Lehman, S. (2000). How animals move: an integrative view. *Science* **288**, 100-106.
Ebashi, S., Endo, M. and Ohtsuki, I. (1969). Control of muscle contraction. *Q. Rev. Biophys.* **2**, 351-384.
Eisenberg, E. and Kielley, W. W. (1970). Native tropomyosin: effect on the interaction of actin with heavy meromyosin and subfragment-1. *Biochem. Biophys. Res. Commun.* **40**, 50-56.
Fawcett, D. and Revel, J. P. (1961). The sarcoplasmic reticulum of a fast-acting fish muscle. *J. Biophys. Biochem. Cytol.* **10**, 89-109.
Fowler, W. and Aebi, U. (1983). A consistent picture of the actin filament related to the orientation of the actin molecule. *J. Cell Biol.* **97**, 264-269.
Franzini-Armstrong, C. (1996). Functional significance of membrane architecture in skeletal and cardiac muscle. *Soc. Gen. Physiol. Ser.* **51**, 3-18.
Fromherz, S. and Szent-Györgyi, A. G. (1995). Role of essential light chain EF hand domain in calcium binding and regulation of scallop myosin. *Proc. Natl. Acad. Sci. USA* **92**, 7652-7656.
Fukunaga, T., Kubo, K., Kawakami, Y., Fukashiro, S., Kanehisa, H. and Maganaris, C. N. (2001). *In vivo* behaviour of human muscle tendon during walking. *Proc. R. Soc. Lond. B. Biol. Sci.* **268**, 229-233.
Gillis, G. B. (1998). Neuromuscular control of anguilliform locomotion: patterns of red and white muscle activity during swimming in the American eel *Anguilla rostrata*. *J. Exp. Biol.* **201**, 3245-3256.
Goldman, D. E. and Hueter, T. F. (1956). Tabular data of the velocity and absorption of high-frequency sound in mammalian tissues. *J. Acoust. Soc. Am.* **28**, 35-37.
Hanson, J. and Lowy, J. (1957). Structure of smooth muscles. *Nature* **180**, 906-909.
Hanson, J. and Lowy, J. (1961). The structure of the muscle fibres in the translucent part of the adductor of the oyster *Crassostrea angulata*. *Proc. R. Soc. Lond. B. Biol. Sci.* **154**, 173-196.
Hanson, J. and Lowy, J. (1964). Comparative studies on the structure of contractile systems. *Circ. Res.* **15**, 4-13.
Hill, A. V. (1938). The heat of shortening and the dynamic constants of muscle. *Proc. R. Soc. Lond. B. Biol. Sci.* **126**, 136-195.
Houdusse, A., Kalabokis, V. N., Himmel, D., Szent-Györgyi, A. G. and Cohen, C. (1999). Atomic structure of scallop myosin subfragment S1 complexed with MgADP: a novel conformation of the myosin head. *Cell* **97**, 459-470.
Houdusse, A., Szent-Györgyi, A. G. and Cohen, C. (2000). Three conformational states of Scallop myosin S1. *Proc. Natl. Acad. Sci. USA* **97**, 11238-11243.
Hoyle, G. (1969). Comparative aspects of muscle. *Ann. Rev. Physiol.* **31**, 43-82.
Huxley, H. E. (1964). Evidence for continuity between the central element of the triads and extracellular space in frog Sartorius. *Nature* **202**, 10676-10771.
Josephson, R. K. (1975). Extensive and intensive factors determining the performance of striated muscle. *J. Exp. Zool.* **194**, 135-154.
Josephson, R. K. (1984). Contraction dynamics of flight and stridulatory muscles of tettigoniid insects. *J. Exp. Biol.* **108**, 77-96.
Kalabokis, V. N. and Szent-Györgyi, A. G. (1997). Cooperativity and regulation of scallop myosin and myosin fragments. *Biochemistry* **36**, 15834-15840.
Kier, W. M. (1985). The musculature of squid arms and tentacles: Ultrastructural evidence for functional differences. *J. Morphol.* **185**, 223-239.
Kier, W. M. and Curtin, N. A. (2002). Fast muscle in squid (*Loligo pealei*): contractile properties of a specialized muscle fibre type. *J. Exp. Biol.* **205**, 1907-1916.
Kier, W. M. and Smith, K. K. (1985). Tongues, tentacles and trunks: the biomechanics of movement in muscular-hydrostats. *J. Linn. Soc. Lond. Zool.* **83**, 307-324.
Kier, W. M. and Thompson, J. T. (2003). Muscle arrangement, function and specialization in recent coleoids. *Berliner Paläobiologische Abhandlungen* **3**, 141-162.
Knapp, M. F. and Mill, P. J. (1971). The contractile mechanism in obliquely striated body wall muscle of the earthworm, *Lumbricus terrestris*. *J. Cell Sci.* **8**, 413-425.
Lännergren, J. (1987). Contractile properties and myosin isoenzymes of various kinds of *Xenopus* twitch muscle fibres. *J. Muscle Res. Cell Motil.* **8**, 260-273.
Lehman, W. and Szent-Györgyi, A. G. (1975). Regulation of muscular *contraction*. Distribution of actin control and myosin control in the animal kingdom. *J. Gen. Physiol.* **66**, 1-30.
Lowy, J. and Millman, B. M. (1962). Mechanical properties of smooth muscles of cephalopod molluscs. *J. Physiol.* **160**, 353-363.
Marsh, R. L. (1990). Deactivation rate and shortening velocity as determinants of contractile frequency. *Am. J. Physiol.* **259**, R223-R230.
Marsh, R. L. and Bennett, A. F. (1985). Thermal dependence of isotonic contractile properties of skeletal muscle and sprint performance in the lizard *Dipsosaurus dorsalis*. *J. Comp. Physiol.* **155**, 541-551.
Marsh, R. L. and Olson, J. M. (1994). Power output of scallop adductor muscle during contractions replicating the *in vivo* mechanical cycle. *J. Exp. Biol.* **193**, 139-156.
Mendelson, M. (1969). Electrical and mechanical characteristics of a very fast lobster muscle. *J. Cell Biol.* **42**, 548-563.
Messenger, J. B., Nixon, M. and Ryan, K. P. (1985). Magnesium chloride as an anesthetic for cephalopods. *Comp. Biochem. Physiol.* **82C**, 203-205.
Milligan, B. J., Curtin, N. A. and Bone, Q. (1997). Contractile properties of obliquely striated muscle from the mantle of squid (*Alloteuthis subulata*) and cuttlefish (*Sepia officinalis*). *J. Exp. Biol.* **200**, 2425-2436.
Millman, B. M. and Bennett, P. M. (1976). Structure of the cross-striated adductor muscle of the scallop. *J. Mol. Biol.* **103**, 439-467.
Morrison, C. M. and Odense, P. H. (1968). Ultrastructure of the striated muscle of the scallop (*Placopecten magellanicus*). *J. Fish. Res. Bd. Can.* **25**, 1339-1345.
Nunzi, M. G. and Franzini-Armstrong, C. (1981). The structure of smooth and striated portions of the adductor muscle of the valves in a scallop. *J. Ultrastruc. Res.* **76**, 134-148.
O'Dor, R. K. (1988). The forces acting on swimming squid. *J. Exp. Biol.* **137**, 421-442.
O'Dor, R. K. and Shadwick, R. E. (1989). Squid, the olympian cephalopods. *J. Ceph. Biol.* **1**, 33-55.
Olson, J. M. and Marsh, R. L. (1993). Contractile properties of the striated adductor muscle in the Bay Scallop *Argopecten irradians* at several temperatures. *J. Exp. Biol.* **176**, 175-193.
Osgood, P. F. and Brewster, W. R. (1963). Effect of temperature and continuous stimulation on gastrocnemius muscle of the frog. *Am. J. Physiol.* **205**, 1299-1303.
Perreault-Micale, C. L., Kalabokis, V. N., Nyitray, L. and Szent-Györgyi, A. G. (1996). Sequence variations in the surface loop near the nucleotide binding site modulate the ATP turnover rates of molluscan myosins. *J. Muscle Res. Cell Motil.* **17**, 543-553.
Rall, J. A. (1981). Mechanics and energetics of contraction in striated muscle of the sea scallop *Placopecten magellanicus*. *J. Physiol.* **321**, 287-295.
Roberts, T. J., Marsh, R. L., Weyand, P. G. and Taylor, C. R. (1997). Muscular force in running turkeys: the economy of minimizing work. *Science* **275**, 1113-1115.
Rome, L. C. and Sosnicki, A. A. (1990). The influence of temperature on mechanics of red muscle in carp. *J. Physiol.* **427**, 151-169.
Rome, L. C., Choi, I., Lutz, G. J. and Sosnicki, A. A. (1992). The influence of temperature on muscle function in fast swimming scup – II. The mechanics of red muscle. *J. Exp. Biol.* **163**, 281-295.
Rosenbluth, J. (1965a). Ultrastructural organization of obliquely striated muscle fibers in *Ascaris lumbricoides*. *J. Cell Biol.* **25**, 495-515.
Rosenbluth, J. (1965b). Smooth muscle: an ultrastructural basis for the dynamics of its contraction. *Science* **148**, 1337-1339.
Rosenbluth, J. (1968). Obliquely striated muscle. IV. Sarcoplasmic reticulum, contractile apparatus, and endomysium of the body muscle of a polychaete, *Glycera,* in relation to its speed. *J. Cell Biol.* **36**, 245-259.
Rosenbluth, J. (1969). Sarcoplasmic reticulum of an unusually fast-acting crustacean muscle. *J. Cell Biol.* **42**, 534-547.
Rosenbluth, J. (1972). Obliquely-striated muscle. In *The Structure and Function of Muscle.* Vol. 1, 2nd edn (ed. G. H. Bourne), pp. 399-420. New York: Academic Press.
Shadwick, R. E., Steffensen, J. F., Katz, S. L. and Knower, T. (1998). Muscle dynamics in fish during steady swimming. *Am. Zool.* **38**, 755-770.
Simmons, R. M. and Szent-Györgyi, A. G. (1978). Reversible loss of calcium control of tension in scallop striated muscle associated with the removal of regulatory light-chains. *Nature* **273**, 62-64.
Simmons, R. M. and Szent-Györgyi, A. G. (1980). Control of tension development in scallop muscle fibres with foreign regulatory light chains. *Nature* **286**, 626-628.

Simmons, R. M. and Szent-Györgyi, A. G. (1985). A mechanical study of regulation in the striated adductor muscle of the scallop. *J. Physiol.* **358**, 47-64.
Szent-Györgyi, A. G. (2007). Regulation by myosin: How calcium regulates some myosins, past and present. In *Regulatory Mechanisms of Striated Muscle Contraction* (ed. S. Ebashi and I. Ohtsuki), pp. 253-264. New York: Springer.
Thompson, J. T., Szczepanski, J. A. and Brody, J. (2008). Mechanical specialization of the obliquely striated circular mantle muscle fibres of the long-finned squid *Doryteuthis pealeii*. *J. Exp. Biol.* **211**, 1463-1474.
Vibert, P. and Castellani, L. (1989). Substructure and accessory proteins in scallop myosin filaments. *J. Cell Biol.* **109**, 539-547.
Wardle, C. S., Videler, J. J. and Altringham, J. D. (1995). Tuning in to fish swimming waves: body form, swimming mode and muscle function. *J. Exp. Biol.* **198**, 1629-1636.
Weber, A. and Murray, J. M. (1973). Molecular control mechanisms in muscle contraction. *Physiol. Rev.* **53**, 612-673.
Wells, C. and Bagshaw, C. R. (1985). Calcium regulation of molluscan myosin ATPase in the absence of actin. *Nature* **313**, 696-697.
Williams, L. W. (1909). *The Anatomy of the Common Squid* Loligo pealii, *Lesueur*. Leiden: EJ Brill.
Xie, X., Harrison, D. H., Schlichting, E., Sweet, R. M., Kalabokis, V. N., Szent-Györgyi, A. G. and Cohen, C. (1994). Structure of the regulatory domain of scallop myosin at 2.8Å resolution. *Nature* **368**, 306-312.
Yang, Y., Kovács, M., Nyitray, L., Reutzel, R., Himmel, D. M., O'Neall-Hennessey, E., Reshetnikova, L., Szent-Györgyi, A. G., Brown, J. H. and Cohen, C. (2007). Rigor-like structures from muscle myosins reveal key mechanical elements in the transduction pathways of this allosteric motor. *Structure* **15**, 553-564.
Young, D. and Josephson, R. K. (1983). Mechanisms of sound-production and muscle contraction kinetics in cicadas. *J. Comp. Physiol.* **152**, 183-195.
Young, J. Z. (1938). The functioning of the giant nerve fibres of the squid. *J. Exp. Biol.* **15**, 170-185.